

Scalable lipid droplet microarray fabrication, validation, and screening

Received 00th January 20xx,
Accepted 00th January 20xx

Tracey N. Bell^{a†} Aubrey E. Kusi-Appiah^{a,b†} Pengfei Lyu^c L. Zhu^d F. Zhu^a David Van Winkle^e Hongyuan Cao^c M. Singh^f and Steven Lenhart^{a*}

DOI: 10.1039/x0xx00000x

High throughput screening of small molecules and natural products is costly, requiring significant amounts of time, reagents, and operating space. Although microarrays have proven effective in the miniaturization of screening for certain biochemical assays, such as nucleic acid hybridization or antibody binding, they are not widely used for drug discovery in cell culture due to the need for cells to internalize lipophilic drug candidates. Lipid droplet microarrays are a promising solution to this problem as they are capable of delivering lipophilic drugs to cells at dosages comparable to solution delivery. However, the scalability of the array fabrication, assay validation, and screening steps has limited the utility of this approach. Here we demonstrate a scalable process for lipid droplet array fabrication, assay validation in cell culture, and drug screening. A nanointaglio printing process has been adapted for use with a printing press. The arrays are stabilized for immersion into aqueous solution using a vapor coating process. In addition to delivery of lipophilic compounds, we found that we are also able to encapsulate and deliver a water-soluble compound in this way. The arrays can be functionalized by extracellular matrix proteins such as collagen prior to cell culture as the mechanism for uptake is based on direct contact with the lipid delivery vehicles rather than diffusion of the drug out of the microarray spots. We demonstrate this method for delivery to 3 different cell types and the screening of 90 natural product extracts on a microarray covering an area of less than 0.1 cm². The arrays are suitable for miniaturized screening, for instance in BSL-3 conditions where space is limited and for applications where cell numbers are limited, such as in functional precision medicine.

Introduction

Cell culture is widely used for biological research, production of biological materials such as antibodies, tissue engineering, and drug discovery. Exposure of cells to a stimulus followed by measurement of a response is the basis of nearly all cell culture experiments. In the case of drug discovery and development, drug candidates are typically dissolved in the solution in which the cells are grown, and the response of the cells to the drug candidates is monitored. In order to maximize the throughput or number of experiments carried out over time, robotic fluid handling systems are widely used with 96, 384, or 1536 well plates at the cell culture site. [1-3] In addition to pipetting drug candidate libraries of more than 100,000 compounds, high throughput screening also requires pipetting of cells, media, and assay reagents in a sterile and precisely controlled biocompatible environment.

Microarrays are a promising solution to increasing the throughput of cell culture screening. They would remove the

fluid handling of the drugs from site of the cell culture, allowing mass production and distribution. The remaining cell culture steps can then be carried out in larger wells, with single pipetting events.

Drug candidates and other small molecules in low abundance would benefit from miniaturization. Screening of hundreds-of-thousands of drug candidates (i.e. high throughput screening) requires costly and cumbersome fluid handling to add cells, reagents, and drug candidates which limits the rate of drug discovery. With drugs needing to be arrayed at the site of cell culture each time, each lab needs a robot. By mass producing arrays at a manufacturing location and distributing them, only one robot is needed saving time and space. In particular, there is a need to overcome these limitations to increase ability to discover drugs in BSL 3/4 labs and for use on primary patient derived cells for functional precision medicine.[3-5] Fabricating microarrays in a lower risk environment is a promising solution to this problem. To miniaturize HTS, small compartments would allow drugs to be screened close together without contaminating each other. Lipids naturally form small compartments and therefore are ideal to solve the technological problem.

Microarray technologies are an established solution to certain fluid handling problems, such as DNA and protein binding assays.[6-12] For instance, DNA hybridization has been scaled up to allow for thousands of hybridization experiments to be carried out on a single surface. Prior to DNA microarray technology, DNA hybridization experiments were carried out by taking variation of DNA strands, labelling them, then heating the mixtures and allowing them to cool and rehybridize.[13] More samples were able to be run by spotting DNA probes then rotating the membrane to get samples to hybridize.[14] Following that, "dot blot hybridizations" used 48 or 96 samples

^a Department of Biological Science and Integrative NanoScience Institute, Florida State University, Biology Unit 1, 89 Chieftan Way, Tallahassee, Florida 32306, United States

^b Viro Research, 2326 Wisteria Drive, Suite 220, Snellville, GA 30078, United States

^c Department of Statistics, Florida State University, 117 N. Woodward Avenue, Tallahassee, FL, 32306

^d Department of Chemistry & Biochemistry, 95 Chieftan Way, Florida State University, Tallahassee, FL 32306-4390

^e Department of Physics, Florida State University, 77 Chieftan Way, Tallahassee, Florida 32306, United States

^f College of Pharmacy and Pharmaceutical Science, Florida A&M University, Tallahassee, FL 32307

† These authors contributed equally to this work

Electronic Supplementary Information (ESI) available: [details of any supplementary information available should be included here]. See DOI: 10.1039/x0xx00000x

* to whom correspondence should be addressed. lenhart@bio.fsu.edu

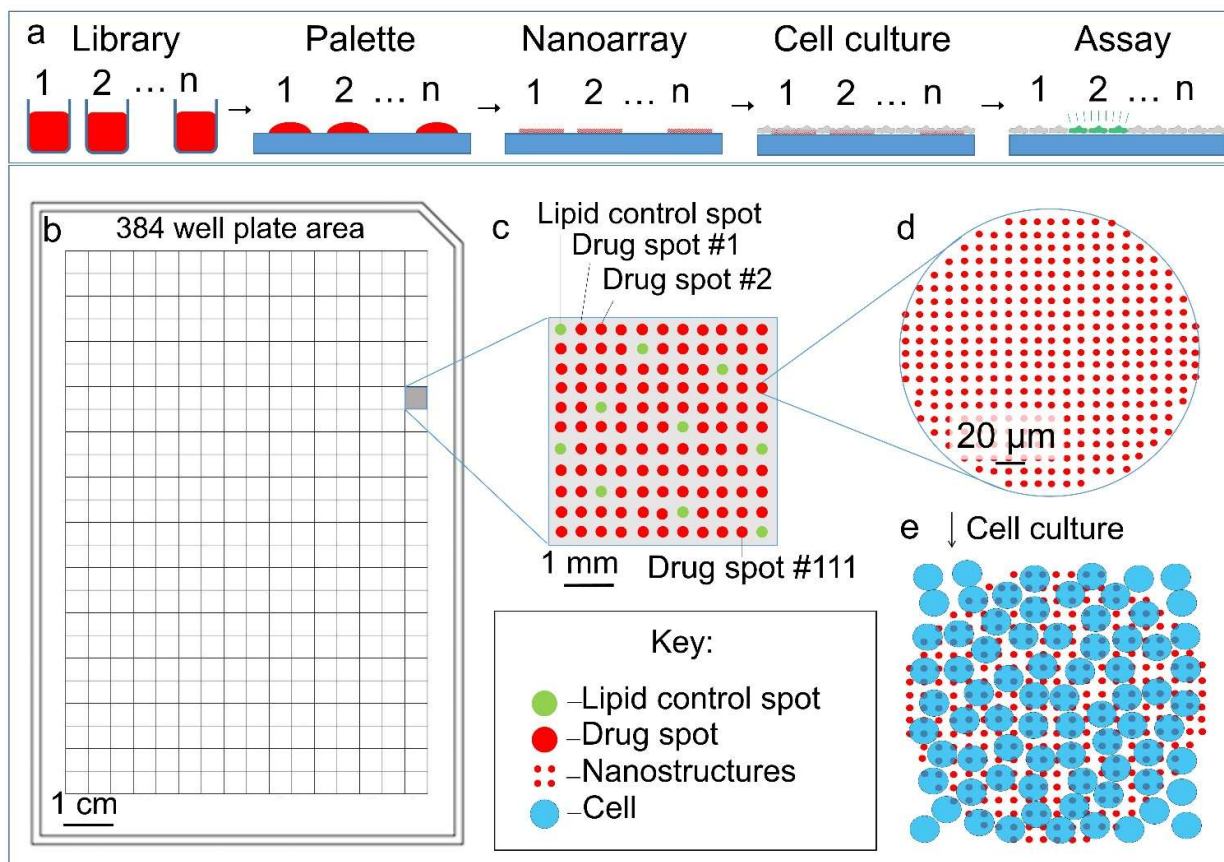


Figure 1. Schematic illustration of the lipid droplet microarray process. (a) A library of therapeutic candidates is dissolved in a solvent. The different candidates are arrayed onto a two-dimensional palette by pin spotting. The palette is used to ink a stamp suitable for forming nanoarrays, which are compatible with cell culture. Cells are cultured on the arrays. Assays are then carried out and used to identify effective therapeutics. (b) Example of a 384 well plate. (c) Millimetre scale of 1 well holding over 100 drugs. (d) Micrometre scale showing the subcellular pattern of individual drug subcellular nanostructures. (e) Cell culture over the microarray.

of bulk DNA to determine a relative quantity of target DNA.[15] Pin spotting is a process that has been developed for a variety of applications that require integration of multiple materials onto the same surface, such as DNA, protein, and polysaccharide microarrays.[16-19] 40,000 different materials can be integrated onto a typical glass slide, overcoming the challenge of individual drug delivery.[18-21] Miniaturization of cell culture has proven more challenging due to difficulties in delivering dosages of different drugs to different cells from a microarray. For instance, covalently linking drugs to surfaces makes it impossible for cells to internalize them.[16, 22, 23] Drug eluting microarrays have been demonstrated for water-soluble drugs.[24-27] In that approach, compounds are encapsulated into a polymer matrix and arrayed on to a surface prior to cell culture. The cellular response to each drug candidate is assayed at each position on the microarray. A challenge with this approach has been the ability to control the dosage, especially in the case of hydrophobic compounds which do not diffuse through water. Furthermore, drug-eluting microarrays are not waterproof, meaning that pre-treatment with coatings such as collagen and washing causes the drugs to

diffuse out of the arrays.[11] These limitations have prevented microarray solutions to high throughput screening problems. Lipid droplet microarrays provide a potential solution by noncovalently attaching lipophilic materials to a surface through encapsulation into lipid droplets.[11, 28-31] Contamination resulting from drug leakage prior to or during cell culture can be avoided with this method as the drugs are not eluted but rather are only taken up by cells upon direct contact with the arrays,[30, 32-34] allowing quantitative dosages similar to solution delivery to be obtained.[35] Lipid droplets of sub-cellular size were found necessary for cell adhesion to the substrates and dosage control.[36] Sub-cellular lipid droplet microarrays have been fabricated using dip-pen nanolithography and polymer pen lithography.[37-39] Here we use a nanointaglio process due to its potential scalability using printing processes.[36, 40] Several aspects of the microarray screening process used here have been described previously (such as pin spotting to create a palette, compatibility with cell culture, delivery of drugs, and quantifying dose response) and are combined and for scalability (Figure 1).[29, 31, 35, 36, 40] The process starts

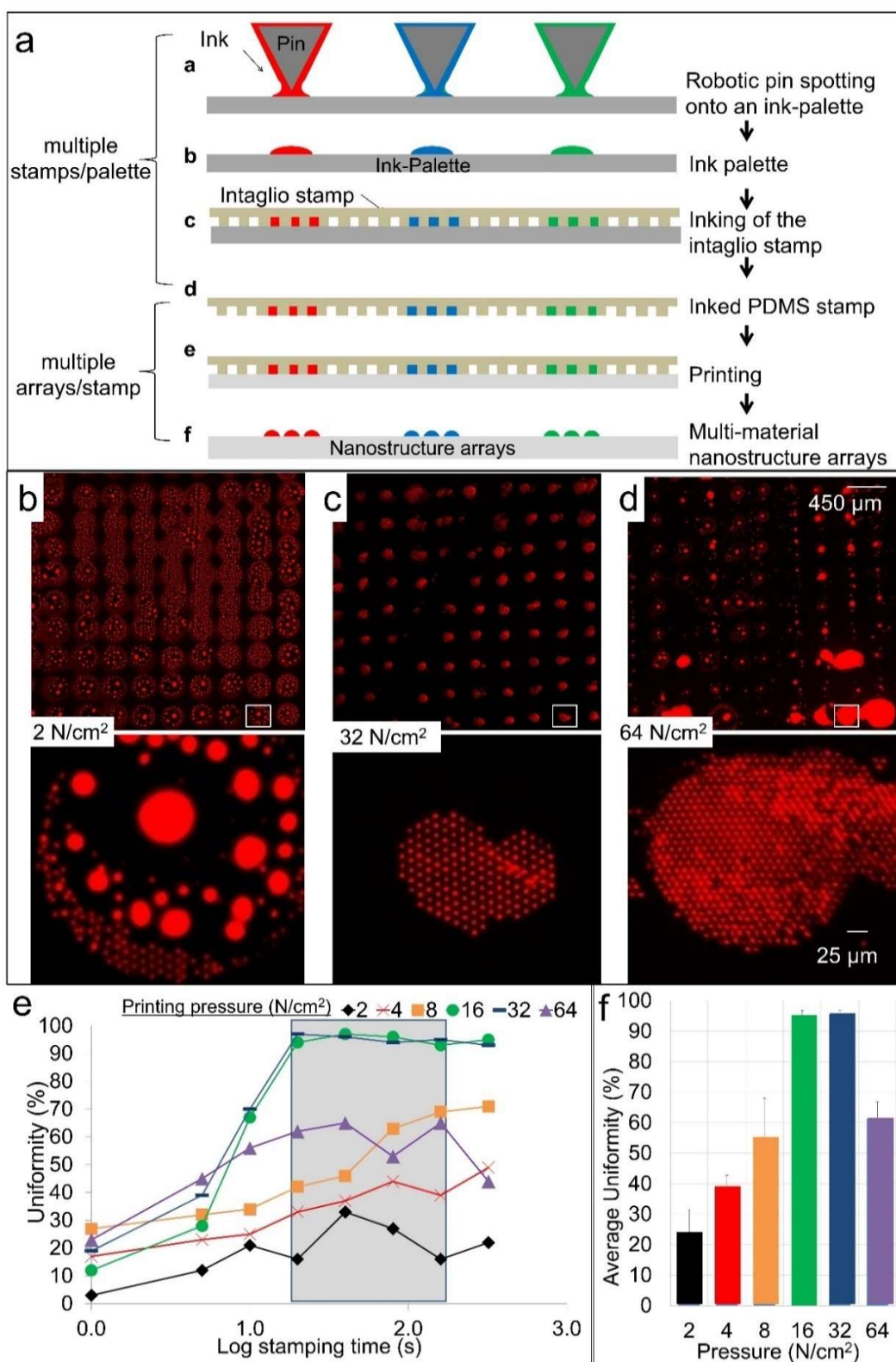


Figure 2. Scalable fabrication of arrays. Fabrication and characterization of nanointaglio microarray using vertical stamping mechanism. (a) A schematic showing the stamping process with the option of using multiple inks, allowing us to scale up by making reproducible copies. (b), (c) and (d) are fluorescence images of arrays with a magnified view of the specific location boxed in white of hexanoic acid / castor oil (hex/cas) droplets stamped using vertical pressures of 2, 32, and 64 N/cm², respectively. Oils were doped with rhodamine-PE for visualization. e) A graph showing the visible individual subcellular nanostructures percentages vs the log of the stamping time in hundreds of seconds the area in grey is the time period of 130-200 seconds. f) A bar graph showing the average uniformity percentage over the span of 130-200 seconds.

with traditional plating by fluid handling in which drug candidates are dissolved in DMSO in 384 well plates. Many libraries are commercially available in this format.[41] Solutions of drug infused lipids are arrayed onto a palette using pin-spotting technology. Typical spot dimensions are 200 μm across spaced 200 μm apart. Spot inhomogeneities likely come from the microarray process and may be improved using inkjet printing.[3, 29] The palettes are used to ink stamps for nanointaglio printing to allow for cell adhesion and controlled dosage to adherent cells.[30, 35, 37] Lipid droplet microarrays require smaller amounts of drugs (nanograms per spot) than solution delivery meaning a single library can be used to make multiple arrays for testing depending on stamp geometry.[35, 36] This process is potentially scalable to allow 46,464 tests, or well-equivalents on the area of a standard microtiter plate (Figure 1b-e).

Results and Discussion

Scalable array fabrication and quality control

Nanointaglio allows for scalable fabrication of the arrays by using a vertical stamping mechanism to create multiple prints from a single pin spotted microarray palette (Figure 2). Using oils doped with rhodamine-PE for visualization, fluorescence images of the droplets were stamped with varying applied pressures. While the spot sizes may not be uniform, we determined an adequate stamping time and printing pressure to acquire repeatable sets of evenly spaced subcellular nanostructures. We define “uniformity” as the percentage of the patterned area that has faithfully transferred individual subcellular nanostructures and dosage is quantified after printing.[34, 35] Printing pressure of 32 N/cm² and stamp times between 13 and 200 seconds were found to be optimal. Spots of different compounds would have diameters of 200 μm and a pitch of 400 μm , therefore a spot density of 625 spots per cm² can be achieved. With printing times on the order of one minute per print, this would allow production of arrays at a throughput of 70 million different compounds per day in a roll-to-roll compatible process.[42] Compound libraries are routinely screened many times, often in different labs as well as in the same lab on different assays, for instance with different cell lines and pathogen strains. Using roll to roll fabrication would

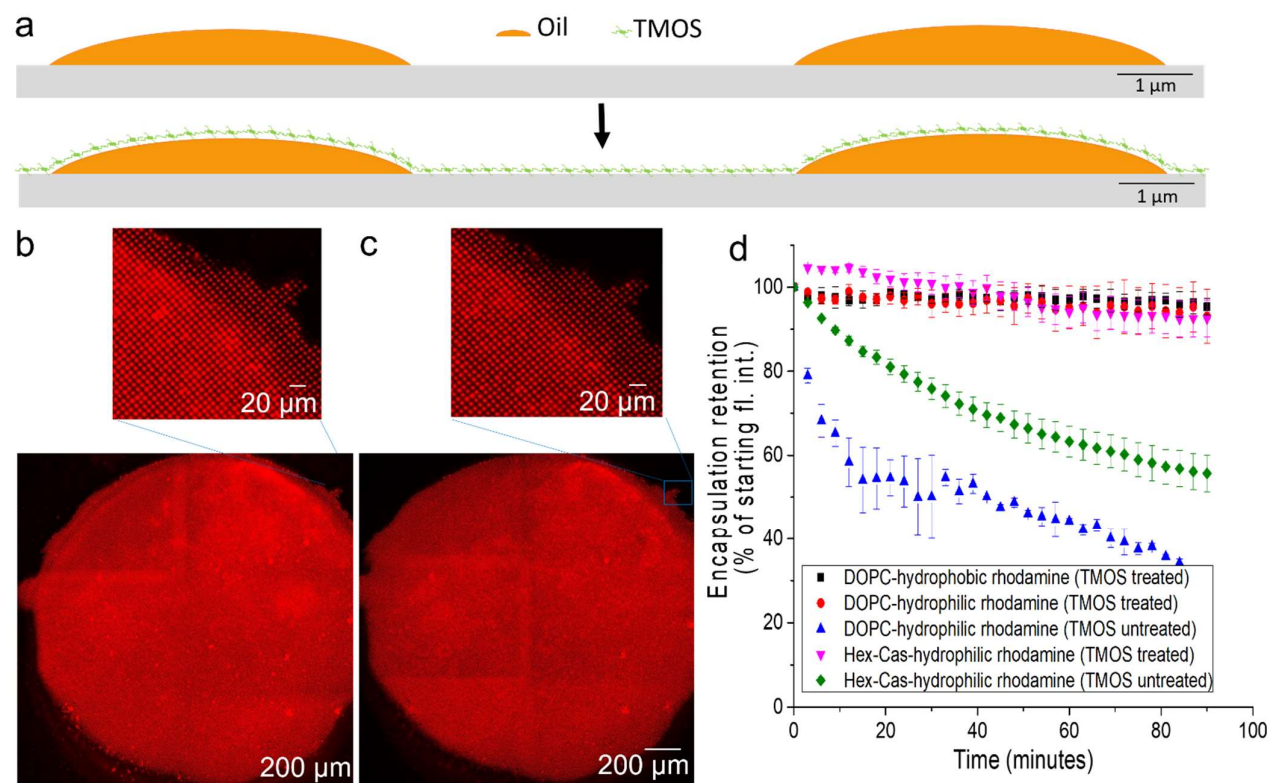


Figure 3 Stable encapsulation using TMOS interaction with oils and phospholipids. a) Schematic showing the top layer of silica-lipid complex of the TMOS treated lipids traps the hydrophilic molecules within the lipid droplet or multilayer and mitigates leakage and disruption during aqueous immersion. b) Fluorescence image of the water-soluble rhodamine B doped mixture of hexanoic acid / castor oil mixture after treatment with TMOS before immersion. At the top is a magnified section showing the subcellular nanostructures within the spot below. (c) Fluorescence image of the water-soluble rhodamine B doped mixture of hexanoic acid / castor oil mixture after treatment with TMOS and immersion under cell culture media for 1 hour. At the top is a magnified section showing the subcellular nanostructures within the spot below. (d) Graph showing a distinct improvement in the stability and resistance to leakage of various oil and phospholipid mixtures when treated with TMOS.

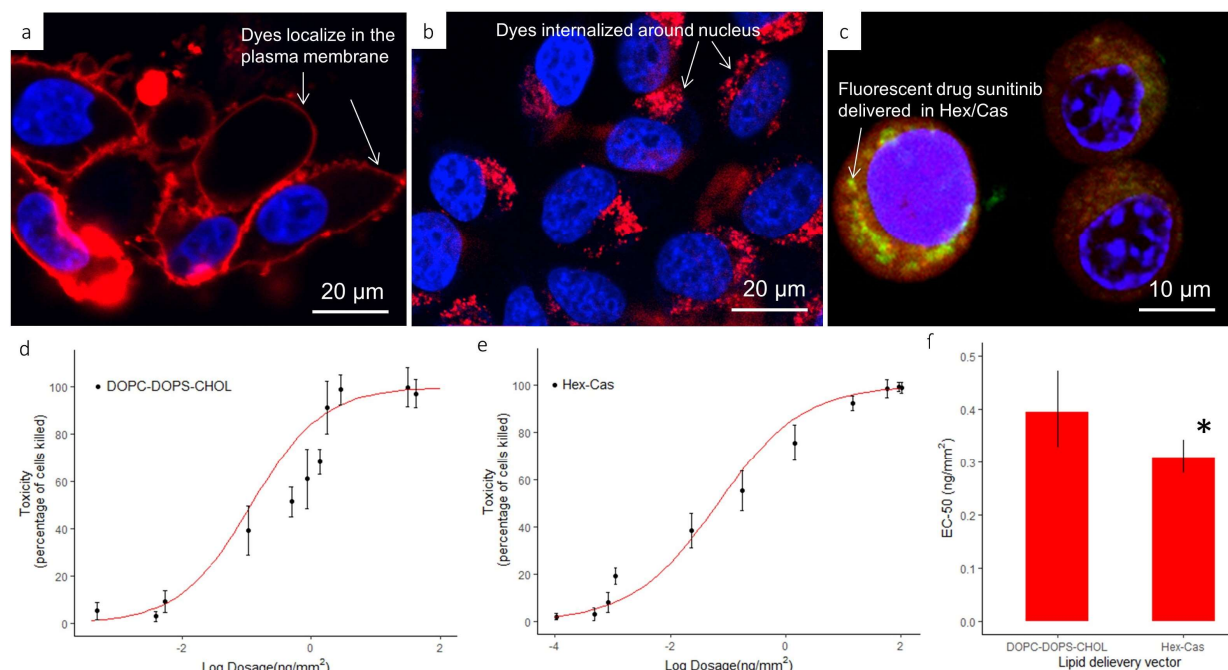


Figure 4. Uptake of hydrophobic small molecules, including a fluorophore and docetaxel. (a) Merged confocal fluorescence image of HeLa cells (blue DAPI stained nuclei) showing localization of rhodamine-PE and docetaxel doped DOPC/DOPS/cholesterol mixture localized in the plasma membrane 12 hours after incubation on array. (b) Merged confocal fluorescence image of HeLa cells showing localization of rhodamine-PE and docetaxel doped castor oil and hexanoic acid mixture localized around the nucleus 12 hours after incubation on array. (c) Merged confocal image showing fluorescent drug sunitinib (green) delivered to HeLa cells from on castor oil and hexanoic acid array. The drug is co-localized with the oil mixture around the nucleus. The image was taken 8 hours after incubation. (d) and (e) Graphs showing the range of toxic effect on HeLa cells when the DOPC/DOPS/cholesterol mixture is used vs the hexanoic acid / castor oil mixture. (f) Graph showing a significantly higher toxic effect on HeLa cells when the oil mixture is used as the delivery vector than when the DOPC/DOPS/cholesterol mixture is used.

allow multiple copies for different labs to test the same compounds, experimental variation, or different assays, with different cell types and strains. Currently libraries are copied into plates, shipped, and tested at multiple facilities. For example, the compounds in the National Center for Advancing Translational Sciences (NCATS) Pharmaceutical Collection (NPC) has been used to screen multiple concentrations, repeated trials, multiple cell lines, follow up studies, etc.[43-47] Nearly 200 peer review articles are currently available that used the NPC.[48, 49]

Although PDMS is convenient for prototype microcontact printing, it is porous and could absorb solvents and small molecules which could change the concentrations of the drug in the droplets. In our case we are quantifying the dosage in terms of fluorescence intensity after printing, which should circumvent this issue. For manufacturing purposes, other polymers such as photocurable perfluoropolyethers (PFPEs) or the thermoplastic polymer cycloolefin copolymer (COC) may be more promising and further improvements of stamp materials can be applied.[50] Such a process would require replenishing of the inks on the stamps. Inkjet printing is a promising approach to high throughput production of the ink palettes.[21]

Use of minimal amounts of reagents could be improved by acoustic droplet ejection technology.[3]

Stable encapsulation of small molecules into lipid droplet arrays

Fluid lipid multilayer patterns on surfaces can be destroyed upon immersion into aqueous solution unless care is taken to prevent this.[30, 34, 36, 38, 51, 52] Previous works have involved careful immersion of phospholipid-based arrays in a low humidity environment and that triglyceride-based formulations can allow more stable immersion.[24, 52, 53] In order to further stabilize the arrays for scalable and portable array-based screening, we have tested a vapor-coating process.[29, 34] In this process, arrays are exposed to tetramethyl orthosilicate (TMOS) vapor, which appears to allow the evaporated lipid film to be fully immersed with cell culture media while maintaining array integrity and without changing morphology to cells or significantly affecting viability. (Supplementary Figure 1)[34] Further experiments would be necessary to conclude on biocompatibility, including proliferative rates and adhesion efficacy. Previous experiments have shown cells can take up rhodamine, as a model drug, within 90 minutes.[36] Since TMOS polymerizes into silica, we

expect that coating the arrays with this process creates a top layer of silica-lipid complex of the TMOS treated lipids that traps encapsulated molecules in the droplet volume, preventing elution of encapsulated small molecules into aqueous solution. (Figure 3a) While it has been shown silicates can be toxic, silicates have been used in drug delivery.[54] Therefore, it is possible that TMOS treatment combined with specific drugs could cause toxicity. TMOS coated arrays were compared against non-TMOS coated arrays to examine the potential toxicity on cells. Non-TMOS coated arrays are prone to “washing away,” therefore blank TMOS coated coverslips were also tested against non-coated blank coverslips to examine the further potential toxicity of TMOS treatment on cells. While further experimentation is necessary, the results showed cells were still viable when grown on the TMOS treatment. (Supplementary Figure 2) The TMOS treatment is not expected to cause significant differences in dosage quantification since the drugs are delivered after coating. Previous experiments have shown encapsulation of several other nonpolar or polar small molecules. We further assessed whether cells can still uptake these materials from the TMOS treated arrays. Figure 3 shows experiments designed to evaluate the ability for TMOS treatment to stabilize oil encapsulated hydrophobic and hydrophilic molecules for in vitro cellular delivery. A lipophilic fluorophore (rhodamine-PE) and a relatively water-soluble fluorophore (rhodamine B) were used as model small molecules to test for stable encapsulation. We found that this process can maintain stable encapsulation of both molecules after immersion into cell culture media, in two different lipid formulations. Without the vapour coating process, the

hydrophilic dye leaks from the drops, while with the TMOS coating it remains stably encapsulated (Figure 3d).

Cellular uptake

Lipid droplets are used to confine reagents, having the drugs suspended in the oil mixture increases cellular uptake of the drug.[30] Lipid droplets with known concentrations are positioned onto a surface, the cells are grown on top of the array of droplets. Cells that do not migrate far are required, when they attach to the surface and over the droplets, the cells fuse with the droplets and adhere to the “empty” surface between droplets. While diffusion is possible, it is unlikely; this fusion is likely by endocytosis, with the cell taking in the lipid nanostructure.[36] We found that cells are still able to internalize encapsulated materials from the arrays after the TMOS treatment process.

Figure 4a-b shows confocal fluorescence data indicating uptake of the hydrophobic fluorophore rhodamine-PE and docetaxel by HeLa cells. Cell nuclei are stained blue with DAPI, while the red signal indicates the localization of rhodamine-PE and docetaxel delivered by TMOS treated DOPC/DOPS/cholesterol in the plasma membrane 12 hours after incubation (Figure 4a). In contrast, Figure 4b shows that a rhodamine-PE and docetaxel doped and TMOS treated castor oil and hexanoic acid mixture delivered the red fluorophore into the cell where it can be seen to be localized around the nucleus 12 hours after incubation (Figure 4b). This shows that the intracellular destination of TMOS treated lipids depends on the delivery material used.[55] One delivery vehicle targets the membrane, while the other targets the cytoplasm. This is important as subcellular

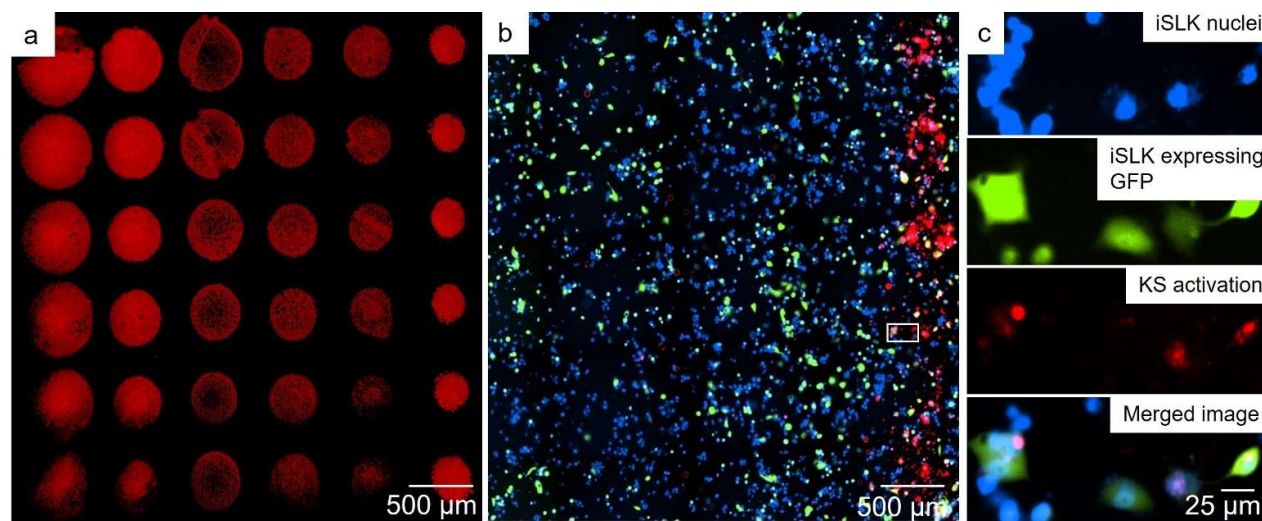


Figure 5. Microarray uptake of a hydrophilic drug. Virus assay In vitro delivery of hydrophilic drugs. (a) Doxycycline activates lytic viral gene expression in Kaposi Sarcoma-associated herpesvirus (KSHV) latently infected (iSLK.219) cells. Fluorescence image of TMOS-treated, rhodamine-PE doped oil mixture (hexanoic acid/castor oil) containing hydrophilic drugs. Rows are different hydrophilic drugs; columns are replicates of the same hydrophilic drugs. The column on the right is doxycycline while the other columns are negative controls. Image gamma corrected. (b) Fluorescence image of iSLK cells cultured over drug patterns for 48 hours. iSLK.219 cells constitutively express GFP; activated cells express RFP only over the doxycycline arrays. Cell nuclei are stained DAPI blue. (c) Zoom in of area in (b) indicated by white box. Cells fluorescing red due to RFP expression from viral activation. High contrast was used for visibility. All micrographs are at 10x magnification (a) and (b) are large images stitched together.

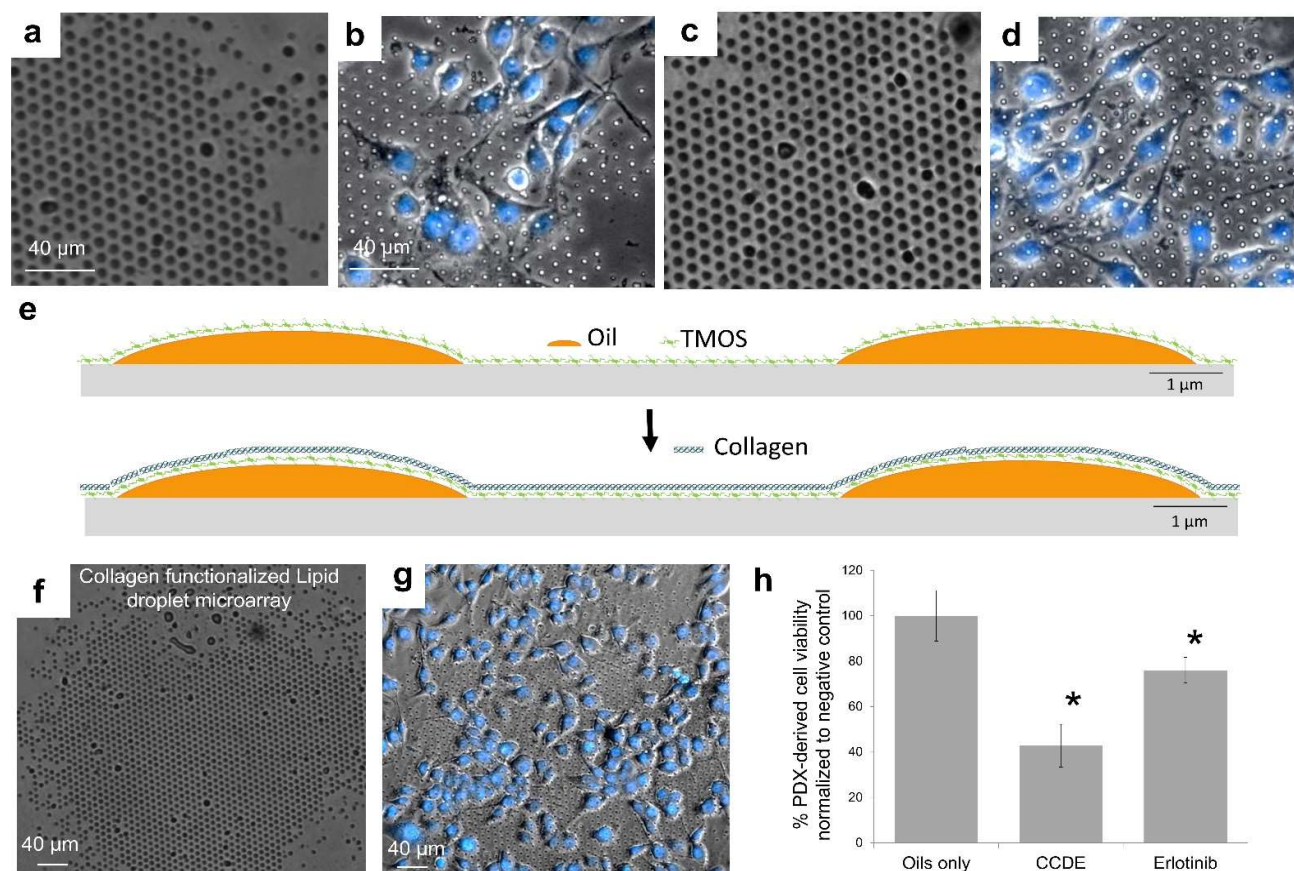


Figure 6. Compatibility with extra cellular matrix coating for primary cell culture. (a) Cell viability of PDX-derived cell line TM00199 after 8 passages in vitro on lipid droplet microarrays. (a) and (c) are phase contrast images of lipid/drug arrays containing the drugs CCDE and Erlotinib, respectively, with each dot representing one droplet, fabricated on collagen coated polystyrene. (b) and (d) are cells cultured over the patterns in (a) and (c) respectively. Cells were washed three times vigorously to remove detached ones and the remaining adherent ones stained with DAPI, with DAPI stained nuclei in blue. The DAPI stained cells are counted as the viable cells over the selected area. Surface coating for adhesion of lung cancer PDCs to lipid droplet microarrays f. Oil (Hex/Cas) array printed on collagen functionalized cell culture polystyrene. (g) Patient derived cells from PDX model line TM00199, passage #8, adhering to the arrays. (h) Cell count over the arrays was normalized to the pure lipid control (oils). *Denotes significantly difference from the control.

localization of drugs has been shown to be related to their activity.[56]

As seen in Figure 4c, there is some variability in the uptake depending on the contact with and location and mobility of the cells on/around the dots when there is not full confluence. While the cell on the left shows an increased uptake amount compared to the other cells that also have green in them but at a lower and differing amount. These will be some of the inherent variations that come with this method when cell seeding is not to confluence. A fluorescent drug, sunitinib, was then delivered to the cells in a hexanoic acid / castor oil mixture (Figure 4c) to determine potency. A standard way to quantify the potency of a drug is to measure the effective concentration with a half maximal response, or EC-50. Lower EC-50 means less drug is needed to cause the same response. The range of toxic effect on HeLa cells when the oil mixture is used as the delivery vector than when the DOPC/DOPS/cholesterol mixture is used is shown in Figure 4d and 4e. A significantly higher potency was observed when the hexanoic acid / castor oil formulation is used

as the delivery vehicle than when the DOPC/DOPS/cholesterol mixture was used (Figure 4f). While formulation is typically optimized after high throughput screening [38, 57] due to limitations in throughput, improved delivery at the high throughput screening stage is a promising approach to repurposing or discovery of potentially therapeutic materials that are incompatible with traditional screening methods such as brick dust molecules.[58-60]

Lipophilic drugs pose a challenge in drug screening, yet such compounds make up 40% of FDA approved oral drugs, and 75% of drug candidates under development.[61, 62] While recent advances in the pharmaceutical industry have made progress in improving the bioavailability of water-soluble drugs, lipophilic based assays remains problematic.[16, 25, 62] For example, when a lipophilic drug is added to water, the actual amount of drug taken up by the cell, if any at all, is often unknown.[35] While microarrays have been used previously for drug delivery to cells, the cells take up the drugs from the array instead of through added solution and they are limited to water-soluble

drugs.[16, 62] While further formulations may be required to deliver varying drugs, our results indicate the suitability for lipid droplet microarrays to quantitatively deliver a lipophilic drug to different parts of a cell.

Assay validation

Before conducting a screening experiment, it is important to validate the assay. This process typically involves testing of a positive control, or a compound that is known to give an efficacious response. We validated two assays, one for viral gene activation with applications in virology, and a second for culture of primary cancer cells with applications in functional precision medicine. An assay for viral activation of latently infected Kaposi Sarcoma-associated herpesvirus (KSHV) was validated using iSLK.219 cells using the water soluble compound doxycycline as the positive control.[63] Treatment of the cells with doxycycline induces viral lytic gene expression as a result of doxycycline-inducible expression of key viral switch gene RTA (Figure 5).[64] High contrast was used for visibility. The cells include a constant GFP and an RFP that fluoresces when the lytic cycle is induced. Using the TMOS-treated, rhodamine-PE doped oil mixture (hexanoic acid/castor oil) containing the hydrophilic drug doxycycline and a control, the doxycycline successfully activated lytic viral gene expression as indicated by expression of RFP under the control of lytic gene promoter.[64-66] Cells cultured over lipid spots that didn't contain the drug (negative controls) did not express the reporter gene. As doxycycline is a water-soluble drug, with a calculated logP of -0.7, [63] its compatibility with lipid droplet microarray delivery in this assay indicates that this approach is not limited to lipophilic compounds. Further tests to determine the range of drug physicochemical properties compatible with this technique are therefore warranted.

Some cell lines require adhesion to the surface, specifically for many patient derived cell lines, so extra cellular matrix coatings are often used in primary cell culture. To verify a patient derived cell line could adhere to the lipid droplet microarrays with a surface coating and successfully deliver drugs, preliminary experiments were carried out with the patient derived cells, TM00199, maintained in PDX models (Figure 6). The lipid/drug arrays containing the anticancer drugs 1-(2-Chlorophenyl)-1-(4-chlorophenyl)-2,2-dichloroethane (CCDE) and Erlotinib were fabricated on collagen coated polystyrene with each dot representing one droplet.[67, 68] Cells were cultured over the patterns and successfully attached to the surface (Figure 6). Cells tend to aggregate over the lipid arrays, so the areas without lipid are lower in cell density, and the negative lipid control sometimes has the highest density, therefore the areas with only lipids were used as the negative control. Once the PDX-derived cell line TM00199 lung cancer PDCs adhered to the lipid droplet microarrays the delivery of drugs to the cells was also effectively demonstrated by both CCDE and Erlotinib having a significantly lower viability than the pure lipid control (oils).

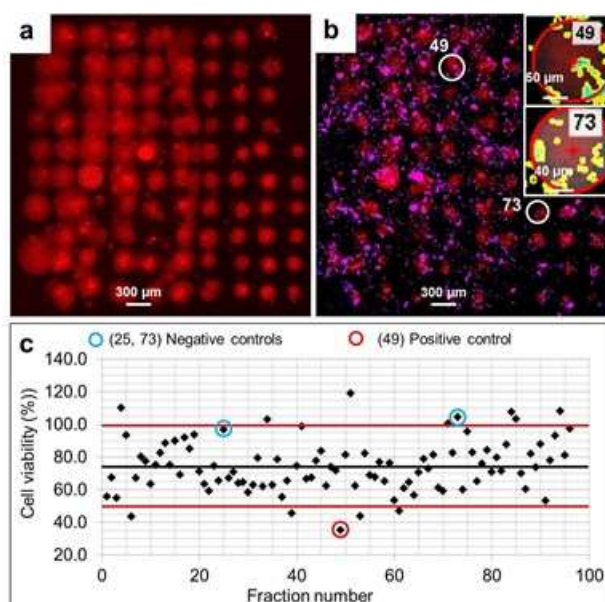


Figure 7. Screening Lipid droplet microarray screening of 92 different natural product extracts for antiproliferative effects on PDX-lung cancer cells. a. Rhodamine-PE doped hexanoic acid/castor oil and extract mixture arrays. b. DAPI stained cells incubated over arrays in (a) for 24 hours. Insets show the cells over white circled areas. (73) is negative control with oil only, (49) is positive control of the anticancer drug erlotinib hydrochloride. c. Graph of cell viability over each of the fractions screened. Grey line indicates mean, viabilities of +/- 1.5 SD are indicated by the red lines as hits in this low throughput screen. Fractions above the top red line are likely to promote cell growth.

Functional precision medicine is based on the idea that cells taken from patient's biopsy can be exposed to drugs *ex vivo* in order to determine optimal responses.[4] Assays such as BH3 profiling have proven effective in determining efficacy in a variety of different cancers.[69-73] High throughput screening has found several small molecules capable of differentiating stem cells.[74] A challenge lies in obtaining enough fresh primary cells to test different therapeutics and/or combinations.[75] One approach is to grow patient derived cells.[69-73] However, it is known that as cells proliferate in culture, adaptation of cells to the artificial environment often results in the cells not responding to drugs as they would in the organism.[76] Lipid droplet microarrays are able to assay the cultured cells quickly after the biopsy, but before they have proliferated and adapted to the cell culture environment. The process of obtaining cells from an organism and keeping them alive in culture requires significant fluid handling steps that make it challenging to carry out in high throughput, especially at scales of more than 50,000 compounds at a time.

Screening

A preliminary test of the suitability for lipid droplet microarray technology to screen a lipophilic natural product library has been carried out as shown in Figure 7. Between 1981 and 2019, approximately 50% of all approved small molecule drugs have

been natural products, natural product derivatives or analogues even though only a negligible fraction of high throughput screening interrogations have used natural products.[77] However, many lipophilic natural products may be missed due to the need for delivery through aqueous solutions. We used the most non-polar fractions of extracts from the US NCI Natural Products Repository library.[78] PDX-lung cancer cells were plated over the arrays and viability was calculated for each spot. Using this method, four hits were obtained with a view to scaling up the process to screen more extracts from the natural product library. It is important to note that Z-scores in screening experiments are not typically used for hypothesis testing, but rather as a method to rank candidates in order to narrow down the possibilities for follow-up investigations. In this case, the low throughput screen is a first test of the technology, and higher throughput screens would have a stricter z-score threshold.[79] Fluid handling remains a limit in the throughput of this assay because the drugs must be added to the formulations prior to arraying. However, upon further scale up of the process described here, arrays can be mass produced from a single set of formulated plates. Since dosages on the order of nanograms per spot are needed, thousands of plates could be manufactured from milligrams of material.

Conclusions

We have presented a scalable microarray screening process that is compatible with compounds of varying physicochemical properties. First a scalable printing nanointaglio printing process has been demonstrated for arrays with controllable dosages. A vapour coating process has been demonstrated that allows for stable immersion into aqueous solution. These arrays can encapsulate lipophilic and water-soluble drugs. Two assays were validated and a preliminary screen of 92 different natural products was carried out. In addition to lowering the cost of high throughput screening and making it accessible to labs, the arrays have potential to overcome limits with current screening technology. The resulting technology has potential for use in BSL 3/4 containment, for use on fresh primary cells from patients, and for generally increasing throughput while decreasing cost of high throughput screening.

Author Contributions

T.B. analysed data and wrote the manuscript together with S.L. A.K.A. carried out all experiments and analysed data with help from all authors. P.L. and H.C. contributed to data analysis. L.Z. contributed to the cellular uptake experiments and F.Z. contributed to the virus activation assay. D.V.W. contributed to experimental design. M. S. contributed to the PDX cell culture experiments. S.L. conceptualized and provided the methodology of and directed experiments.

Conflicts of interest

There are no conflicts to declare.

Acknowledgements

The US NCI Natural Products Repository library was kindly provided by Barry O'Keefe at the Frederick National Laboratory for Cancer Research. The authors thank Troy W. Lowry, James Penate, Cecelia Bouaichi, and Parker Pecina, for help with the array fabrication and Javier Mariscal and Juan Reza for reviewing the paper.

Materials and Methods:

Nanointaglio array fabrication:

Printing solution formulation and micro arraying:

1,2-dioleoyl-sn-glycero-3-phosphocholine (DOPC) and 1,2-dimyristoyl-sn-glycero-3-phosphoethanolamine-N- (lissamine rhodamine-B-sulfonyl) (ammonium salt) or rhodamine-PE dissolved in chloroform were purchased from Avanti Polar Lipids, aliquoted into a glass vial and dried in a vacuum. Rhodamine-PE was used to dope the DOPC for fluorescence visualization and characterization. Deionized water was added to the vials containing the dried lipids to form liposomes. The samples were sonicated for 10 minutes and aliquoted into microtiter plates. The liposomes were then microarrayed using an Arrayit SpotBot pinspotter, onto a flat polydimethylsiloxane (PDMS) pallet and dried in a vacuum for 2 hours.

For the intracellular localization of lipids experiment formulations of rhodamine-PE doped DOPC/DOPS/cholesterol and Hexanoic Acid-Castor oil were printed and stamped onto glass bottom dishes.

Hand stamping method:

A polydimethylsiloxane (PDMS) stamp with well features of 5 μm diameter and 2.5 μm depth was inked by pressing the patterned surface onto the ink palette. The inked stamp was then pressed onto polystyrene or glass cell culture surface with the thumb to obtain spots made up of smaller subcellular nanostructures with ~ 5 μm lateral dimensions.

Vertical stamping method:

A vertical press system was designed to be used for weight dependent stamping of the arrays. The vertical press system involves a top-down press system using controlled pressure for small well plates. A 1cm thick PDMS stamp with well features of 5 μm diameter and 2.5 μm depth on one surface were fabricated for vertical printing and inked with the array by gently pressing the surface with the wells over the array on the PDMS pallet. The inked

stamp was then affixed to a flat rigid plastic backing. The stamp was then pressed to the well plate culture surface. Weights generating forces ranging from 1N-16N were applied to the stamp.

Rolling press method:

A 3mm thick PDMS stamp with well features of 5 μm diameter and 2.5 μm depth on one surface were fabricated for rolling press printing. The PDMS was affixed to a roller with the side with the well features facing outward. The stamped was inked with the arrays by gently rolling the affixed stamp over the microarrayed pallet making sure the stamps were aligned to capture all the array spots. The inked roller stamp was then gently rolled over the cell culture glass surface to produce the nanointaglio arrays.

Microscopy:

Optical microscopy:

Epifluorescence microscopy was done using a Ti-E inverted microscope (Nikon Instruments, Melville, NY, USA) fitted with a Retiga SRV (QImaging, Surrey, BC, Canada) CCD camera (1.4 MP, Peltier cooled to $-45\text{ }^{\circ}\text{C}$). Rhodamine-PE doped lipid structures were imaged using the G-2E/C filter. DAPI was imaged using the UV-2E/C fluorescence filter, and GFP were imaged using the B-2E/C. Confocal microscopy was carried out on an Olympus FV1000 Confocal Laser Scanning Biological Microscope. A 60x oil objective and a 405-nm diode laser (for DAPI) or a 543-nm He/Ne laser (for rhodamine) was used.

The fabricated arrays were characterized using optical fluorescence microscopy. For the 90-extract screen we used a single dosage of 1.2 pg/mm^2 +/- 20% as determined by fluorescence calibration.

Atomic force microscopy:

AFM heights of the lipid prints were measured in tapping mode with a Dimension Icon AFM (Bruker, Billerica, MA, USA) and tapping mode AFM cantilevers (FESPA, 8 nm nominal tip radius, 10-15 μm tip height, 2.8 N/ m-1 spring constant, Bruker, Billerica, MA, USA).

Dye encapsulation and leakage:

Two dyes, hydrophilic rhodamine B and hydrophobic rhodamine-PE, were each mixed separately with DOPC and with a mixture of castor oil and hexanoic acid and used for the fabrication of nanointaglio arrays. In at least 4 array samples, each mixture of DOPC/rhodamine B, DOPC/rhodamine-PE, hexanoic acid / castor oil / rhodamine B and hexanoic acid / castor oil / rhodamine-PE were fabricated. Half the samples were treated with TMOS, and the other half were left untreated. Both TMOS treated and untreated microarrays were immersed under cell culture media and a fluorescence microscopy time lapse taken to record the change in fluorescence intensity over the period of 90 minutes. The relative change in fluorescence intensity as a percent of the starting intensity was plotted as a measure of dye leakage.

Surface Treatments

TMOS treatment:

Two glass vials, one containing 2mL of tetramethyl Orthosilicate, purchased from Sigma Aldrich® and the other containing deionized water were placed into a larger sealable glass container. The lipid multilayers were placed in the larger glass container with the other two vials. The container was then sealed tight and left at room temperature for 4 hours after which the printed lipids were removed and ready for cell culture.

Collagen coating:

To ensure proper coating, 200 μL of 0.01% collagen was aliquoted onto culture substrate and incubated for 2 hours at 37 $^{\circ}\text{C}$. Collagen solution was aspirated off culture substrate and surface washed 3X in HBSS buffer. The substrate was air dried under sterile conditions for 1 hour before the lipid array was then stamped onto the collagen coated surface. Some arrays were treated with TMOS vapor for 4 hours. TMOS treated arrays were immersed under another 200 μL of 0.01 collagen solution for 2 hours at 37 $^{\circ}\text{C}$. Collagen solution was aspirated off the array and washed 3X with HBSS buffer.

PLL coating:

Poly-l-lysine purchased from Sigma (P6407-5MG) was used to coat slides to promote cell adhesion. The poly-l-lysine was thawed to room temperature and a 1:10 dilution was made in deionized water; the slides were placed inside solution for 5 minutes and left to dry in the oven at 60 degrees Celsius for one hour.

Cell culture:

The cell types used included HeLa cells purchased from ATCC. iSLK.219 cells were obtained from Jinjong Myoung and cultured as previously described. [65, 66] PDX cells used in these experiments were cultured from PDX lung tumours, TM 0199 (Jackson Labs). These cells express EGFR L858R mutations. For the intracellular localization of lipids experiment the cells were incubated for 6 hours, stained with DAPI, and then imaged using confocal microscopy to determine the intracellular location of the lipids. Microarrays were immersed under cell culture media without cells. The cells were then added onto the already immersed arrays. Cells were incubated over arrays for the times shown below.

TMOS toxicity measurements:

TMOS coated arrays were compared against non-TMOS coated arrays to examine the potential toxicity on cells. Non-TMOS coated arrays are prone to "washing away," therefore blank TMOS coated coverslips were also tested against non-coated blank coverslips to examine the further potential toxicity of TMOS treatment on cells. The Invitrogen™ LIVE/DEAD™ Cell Imaging Kit (488/570) was purchased from Thermo Fisher Scientific. Micrographs were taken

Rhodamine-PE doped lipid structures and dead cells were imaged using the G-2E/C filter and GFP were imaged using the B-2E/C filter. The results were merged and transferred to ImageJ software. A ROI was placed over each droplet in the TMOS treated and untreated samples, and the number of dead cells vs live cells counted. The process was repeated over blank areas.

Cell viability measurements:

For EC50 determinations, the lipid/drug mixtures were stamped multiple times into cell culture wells to obtain the variation in quantities (heights) lipid/drugs deposited. The heights were converted to dosages using the calibration method described previously.[80, 81] Cells were cultured for 24 hours in all viability tests. Cells were washed three times vigorously to remove detached ones and the remaining adherent ones stained with DAPI. The DAPI stained cells are counted as the viable cells over the selected area. Dose response curves were plotted in Origin and EC50 values extracted from the plots. Toxicity experiments were done in triplicate with 3 repeats and error bars represent standard deviation from the nine experiments.

The arrays were fluorescently imaged using the Texas red filter of the Nikon Eclipse Ti microscope. For optical calibration purposes the images were taken, and fluorescence intensities images were taken with an exposure time ranging from 2 microseconds to 2 seconds. AFM measurements of the imaged fluorescent docetaxel lipid multilayers were taken. Calibration was done using as previously described.[37]

Natural product extracts:

90 natural product extract fractions dissolved in DMSO obtained from the NCI at Frederick National Laboratory for Cancer Research were mixed with 1,2-dimyristoyl-sn-glycero-3-phosphoethanolamine-N- (lissamine rhodamine-B-sulfonyl) (ammonium salt) were used.[41] 90 of the most non-polar fractions of extracts (Acetone (ACN) / dichloromethane (DCM), and methanol (MeOH) / DCM fractions) were mixed with (rhodamine-PE) doped oil mixture (castor oil and hexanoic acid) in a 384 microtiter well plate. Three control wells, two negative controls with only DMSO and a positive control of Erlotinib, were added to the microwells for micro arraying. Mixing of extracts/drugs with oils was done by pipetting up and down. The microtiter plate was then placed in a SpotBot® Extreme pinspotter microarrayer for printing. A 10X10 array design was used to print the array onto a 1mm thick polydimethylsiloxane PDMS pallet. Dwell time of 1s was used for printing. The printed array pallet was placed in a vacuum overnight for drying out the DMSO before nanointaglio stamping. Mixing of other drugs (CCDE, doxycycline) with oils for printing was done in the same fashion. The most non-polar fractions of extracts from the US NCI Natural Products Repository library were used. Acetone (ACN) / dichloromethane (DCM), and methanol (MeOH) / DCM fractions were mixed with the oil carrier (hexanoic acid / castor oil mixture in 1:1 ratio), doped with rhodamine-PE and used for

the screen. We performed the screen at a single dosage of 1.2 pg/mm² +/- 20% as determined by fluorescence calibration. PDX-lung cancer cells were plated over the arrays for 24 hours, washed, stained with DAPI, and then counted. Viability was calculated for each spot and significance assigned to values more than 1.5 standard deviation above or below the population mean (74.5). Using the lipid droplet microarray 92 natural product extracts were screened, with two negative controls and a positive control (Figure 7). With a negative control set to a cell viability of 100 percent and a hit was considered if +/-1.5 standard deviations. Four hits were attributed to this screen.

References

1. Michael, S., et al., *A robotic platform for quantitative high-throughput screening*. Assay and drug development technologies, 2008. **6**(5): p. 637-657.
2. Comley, J., *Tools and technologies that facilitate automated screening*. High-Throughput Screening in Drug Discovery, 2006. **35**: p. 37-73.
3. Ellson, R., et al., *Transfer of low nanoliter volumes between microplates using focused acoustics?automation considerations*. Journal of the Association for Laboratory Automation, 2003. **8**(5): p. 29-34.
4. Letai, A., *Functional precision cancer medicine—moving beyond pure genomics*. Nature Medicine, 2017. **23**(9): p. 1028-1035.
5. Collins, F.S. and P. Stoffels, *Accelerating COVID-19 Therapeutic Interventions and Vaccines (ACTIV)*. JAMA, 2020. **323**(24): p. 2455.
6. Yang, M., et al., *Genome-wide microarray analysis of TGFbeta signaling in the Drosophila brain*. BMC developmental biology, 2004. **4**: p. 14-14.
7. Ramanathan, R., et al., *Microarray-based analysis of differential gene expression between infective and noninfective larvae of Strongyloides stercoralis*. PLoS neglected tropical diseases, 2011. **5**(5): p. e1039-e1039.
8. Yang, L., et al., *High-Throughput Methods in the Discovery and Study of Biomaterials and Materiobiology*. Chem Rev, 2021. **121**(8): p. 4561-4677.
9. Cahill, D.J., *Protein and antibody arrays and their medical applications*. Journal of Immunological Methods, 2001. **250**(1): p. 81-91.
10. Hook, A.L., H. Thissen, and N.H. Voelcker, *Surface manipulation of biomolecules for cell microarray applications*. Trends in Biotechnology, 2006. **24**(10): p. 471-477.
11. Howbrook, D.N., et al., *Developments in microarray technologies*. Drug Discovery Today, 2003. **8**(14): p. 642-651.
12. Ma, H. and K.Y. Horiuchi, *Chemical microarray: a new tool for drug screening and discovery*. Drug Discovery Today, 2006. **11**(13): p. 661-668.
13. Taub, F.E., J.M. DeLeo, and E.B. Thompson, *Sequential Comparative Hybridizations Analyzed by Computerized Image Processing Can Identify and Quantitate Regulated RNAs*. DNA, 1983. **2**(4): p. 309-327.

14. Brown, T., *Dot and Slot Blotting of DNA*. Current Protocols in Molecular Biology, 1993. **21**(1): p. 2.9.15-2.9.20.
15. Bhat, A.I. and G.P. Rao, *Dot-blot hybridization technique*, in *Characterization of Plant Viruses*. 2020, Springer. p. 303-321.
16. Köhn, M., et al., *Staudinger Ligation: A New Immobilization Strategy for the Preparation of Small-Molecule Arrays*. Angewandte Chemie International Edition, 2003. **42**(47): p. 5830-5834.
17. Lenhert, S., *Adhesion of Lipid Multilayer Micro- and Nano-Structures Fabricated by Dip-Pen Nanolithography*. Biophysical Journal, 2011. **100**(3): p. 507-507.
18. Gosalia, D.N. and S.L. Diamond, *Printing chemical libraries on microarrays for fluid phase nanoliter reactions*. Proceedings of the National Academy of Sciences, 2003. **100**(15): p. 8721-8726.
19. Popova, A.A., et al., *Droplet-microarray on superhydrophobic-superhydrophilic patterns for high-throughput live cell screenings*. RSC Advances, 2016. **6**(44): p. 38263-38276.
20. Mugerli, L., et al., *In Situ Assembly and Screening of Enzyme Inhibitors with Surface-Tension Microarrays*. Angewandte Chemie, 2009. **121**(41): p. 7775-7780.
21. Sun, Y., et al., *Droplet-in-oil array for picoliter-scale analysis based on sequential inkjet printing*. Lab on a Chip, 2015. **15**(11): p. 2429-2436.
22. Tanaka, M. and E. Sackmann, *Polymer-supported membranes as models of the cell surface*. Nature, 2005. **437**(7059): p. 656-663.
23. Fang, Y., A.G. Frutos, and J. Lahiri, *Ganglioside Microarrays for Toxin Detection*. Langmuir, 2003. **19**(5): p. 1500-1505.
24. Peng, B., et al., *MSN-on-a-Chip: Cell-Based Screenings Made Possible on a Small-Molecule Microarray of Native Natural Products*. ChemBiochem, 2018. **19**(9): p. 986-996.
25. Bailey, S.N., D.M. Sabatini, and B.R. Stockwell, *Microarrays of small molecules embedded in biodegradable polymers for use in mammalian cell-based screens*. Proceedings of the National Academy of Sciences of the United States of America, 2004. **101**(46): p. 16144-16149.
26. Carstens, M.R., et al., *Drug-eluting microarrays to identify effective chemotherapeutic combinations targeting patient-derived cancer stem cells*. Proceedings of the National Academy of Sciences, 2015. **112**(28): p. 8732-8737.
27. Kwon, C.H., et al., *Drug-eluting microarrays for cell-based screening of chemical-induced apoptosis*. Anal Chem, 2011. **83**(11): p. 4118-25.
28. Nii, T. and F. Ishii, *Encapsulation efficiency of water-soluble and insoluble drugs in liposomes prepared by the microencapsulation vesicle method*. International Journal of Pharmaceutics, 2005. **298**(1): p. 198-205.
29. Ghazanfari, L. and S. Lenhert, *Screening of Lipid Composition for Scalable Fabrication of Solvent-Free Lipid Microarrays*. Front Mater, 2016. **3**.
30. Kusi-Appiah, A.E., et al., *Lipid multilayer microarrays for in vitro liposomal drug delivery and screening*. Biomaterials, 2012. **33**(16): p. 4187-94.
31. Nafday, O.A., T.W. Lowry, and S. Lenhert, *Multifunctional lipid multilayer stamping*. Small, 2012. **8**(7): p. 1021-8.
32. Xu, F., et al., *Microengineering methods for cell-based microarrays and high-throughput drug-screening applications*. Biofabrication, 2011. **3**(3): p. 034101.
33. Hook, A.L., H. Thissen, and N.H. Voelcker, *Advanced Substrate Fabrication for Cell Microarrays*. Biomacromolecules, 2009. **10**(3): p. 573-579.
34. Kusi-Appiah, A.E., et al., *Fluid Lipid Multilayer Stabilization by Tetraethyl Orthosilicate for Underwater AFM Characterization and Cell Culture Applications*. MRS Advances, 2017. **2**(57): p. 3553-3558.
35. Kusi-Appiah, A.E., et al., *Quantitative dose-response curves from subcellular lipid multilayer microarrays*. Lab Chip, 2015. **15**(16): p. 3397-404.
36. Lowry, T.W., et al., *Materials Integration by Nanointaglio*. Adv Mater Interfaces, 2014. **1**(4).
37. Nafday, O.A. and S. Lenhert, *High-throughput optical quality control of lipid multilayers fabricated by dip-pen nanolithography*. Nanotechnology, 2011. **22**(22): p. 225301.
38. Lenhert, S., et al., *Massively parallel dip-pen nanolithography of heterogeneous supported phospholipid multilayer patterns*. Small, 2007. **3**(1): p. 71-5.
39. Hirtz, M., et al., *Functional lipid assemblies by dip-pen nanolithography and polymer pen lithography*. Soft Matter Nanotechnology: From Structure to Function, 2015: p. 161-186.
40. Lowry, T.W., et al., *Lipid Multilayer Grating Arrays Integrated by Nanointaglio for Vapor Sensing by an Optical Nose*. Sensors (Basel), 2015. **15**(8): p. 20863-72.
41. Thornburg, C.C., et al., *NCI Program for Natural Product Discovery: A Publicly-Accessible Library of Natural Product Fractions for High-Throughput Screening*. ACS Chem Biol, 2018. **13**(9): p. 2484-2497.
42. Xu, J., et al., *Future of the Particle Replication in Nonwetting Templates (PRINT) Technology*. Angewandte Chemie-International Edition, 2013. **52**(26): p. 6580-6589.
43. Dahlin, J.L., et al., *A Cell-Free Fluorometric High-Throughput Screen for Inhibitors of Rtt109-Catalyzed Histone Acetylation*. PLoS ONE, 2013. **8**(11): p. e78877.
44. Freitas, J., et al., *Identification of Thyroid Hormone Receptor Active Compounds Using a Quantitative High-Throughput Screening Platform*. Current Chemical Genomics and Translational Medicine, 2014. **8**(1): p. 36-46.
45. Hua, Y., et al., *High-Content Positional Biosensor Screening Assay for Compounds to Prevent or Disrupt Androgen Receptor and Transcriptional Intermediary Factor 2 Protein-Protein Interactions*. ASSAY and Drug Development Technologies, 2014. **12**(7): p. 395-418.
46. Schulz, M.M.P., et al., *Phenotype-based high-content chemical library screening identifies statins as inhibitors of in vivo lymphangiogenesis*. Proceedings of the National Academy of Sciences, 2012. **109**(40): p. E2665-E2674.
47. Vliet, S.M., T.C. Ho, and D.C. Volz, *Behavioral screening of the LOPAC1280 library in zebrafish embryos*. Toxicology and Applied Pharmacology, 2017. **329**: p. 241-248.
48. Bialkowska, A.B., et al., *Identification of novel small-molecule compounds that inhibit the proliferative Krüppel-like factor 5 in colorectal cancer cells by high-throughput screening*. Molecular Cancer Therapeutics, 2009. **8**(3): p. 563-570.
49. Casson, L., et al., *Inhibition of Ceramide Metabolism Sensitizes Human Leukemia Cells to Inhibition of BCL2-Like Proteins*. PLoS ONE, 2013. **8**(1): p. e54525.
50. Mukhopadhyay, R., *When PDMS isn't the best*. Analytical Chemistry, 2007. **79**(9): p. 3248-3253.

51. Sanii, B. and A.N. Parikh, *Surface-energy dependent spreading of lipid monolayers and bilayers*. *Soft Matter*, 2007. **3**(8): p. 974-977.
52. Gupta, G., et al., *Stable and Fluid Multilayer Phospholipid-Silica Thin Films: Mimicking Active Multi-lamellar Biological Assemblies*. *ACS Nano*, 2013. **7**(6): p. 5300-5307.
53. Wang, L., M. Schönhoff, and H. Möhwald, *Swelling of Polyelectrolyte Multilayer-Supported Lipid Layers. 1. Layer Stability and Lateral Diffusion*. *The Journal of Physical Chemistry B*, 2004. **108**(15): p. 4767-4774.
54. Korteso, P., et al., *Sol-gel-processed sintered silica xerogel as a carrier in controlled drug delivery*. *Journal of Biomedical Materials Research*, 1999. **44**(2): p. 162-167.
55. Kumar, A., et al., *Multifunctional magnetic nanoparticles for targeted delivery*. *Nanomedicine: Nanotechnology, Biology and Medicine*, 2010. **6**(1): p. 64-69.
56. Klein, I.A., et al., *Partitioning of cancer therapeutics in nuclear condensates*. *Science*, 2020. **368**(6497): p. 1386-+.
57. Feeney, O.M., et al., *50 years of oral lipid-based formulations: Provenance, progress and future perspectives*. *Advanced Drug Delivery Reviews*, 2016. **101**: p. 167-194.
58. Koehl, N.J., et al., *New Insights into Using Lipid Based Suspensions for "Brick Dust" Molecules: Case Study of Nilotinib*. *Pharmaceutical Research*, 2019. **36**(4): p. 13.
59. Gregoriadis, G., *Engineering liposomes for drug delivery: progress and problems*. *Trends Biotechnol*, 1995. **13**(12): p. 527-37.
60. Koren, E. and V.P. Torchilin, *Drug carriers for vascular drug delivery*. *IUBMB Life*, 2011. **63**(8): p. 586-595.
61. Kalepu, S. and V. Nekkanti, *Insoluble drug delivery strategies: review of recent advances and business prospects*. *Acta Pharm Sin B*, 2015. **5**(5): p. 442-53.
62. Rodriguez-Aller, M., et al., *Strategies for formulating and delivering poorly water-soluble drugs*. *Journal of Drug Delivery Science and Technology*, 2015. **30**: p. 342-351.
63. *National Center for Biotechnology Information. PubChem Compound Summary for CID 54671203, Doxycycline*. <https://pubchem.ncbi.nlm.nih.gov/compound/Doxycycline>. Accessed Aug. 30, 2021.
64. Bergson, S., et al., *Fluorescent tagging and cellular distribution of the Kaposi's sarcoma-associated herpesvirus ORF45 tegument protein*. *Journal of virology*, 2014. **88**(21): p. 12839-12852.
65. Myoung, J. and D. Ganem, *Generation of a doxycycline-inducible KSHV producer cell line of endothelial origin: maintenance of tight latency with efficient reactivation upon induction*. *J Virol Methods*, 2011. **174**(1-2): p. 12-21.
66. Sexton, B.S., et al., *Hierarchical regulation of the genome: global changes in nucleosome organization potentiate genome response*. *Oncotarget*, 2016. **7**(6): p. 6460-75.
67. Pérez-Soler, R., et al., *Determinants of tumor response and survival with erlotinib in patients with non-small-cell lung cancer*. *Journal of clinical oncology*, 2004. **22**(16): p. 3238-3247.
68. Scagliotti, G.V., et al., *Sunitinib Plus Erlotinib Versus Placebo Plus Erlotinib in Patients With Previously Treated Advanced Non-Small-Cell Lung Cancer: A Phase III Trial*. *Journal of Clinical Oncology*, 2012. **30**(17): p. 2070-2078.
69. Rys, R.N., et al., *Apoptotic Blocks in Primary Non-Hodgkin B Cell Lymphomas Identified by BH3 Profiling*. *Cancers*, 2021. **13**(5): p. 1002.
70. Jenson, J.M., et al., *Epistatic mutations in PUMA BH3 drive an alternate binding mode to potently and selectively inhibit anti-apoptotic Bfl-1*. *eLife*, 2017. **6**: p. e25541.
71. Kale, J., et al., *Phosphorylation switches Bax from promoting to inhibiting apoptosis thereby increasing drug resistance*. *EMBO reports*, 2018. **19**(9): p. e45235.
72. Grundy, M., et al., *Predicting effective pro-apoptotic anti-leukaemic drug combinations using co-operative dynamic BH3 profiling*. *PloS one*, 2018. **13**(1): p. e0190682-e0190682.
73. Potter, D.S., et al., *Dynamic BH3 profiling identifies active BH3 mimetic combinations in non-small cell lung cancer*. *Cell Death & Disease*, 2021. **12**(8): p. 741.
74. Chen, S., *Screening-Based Chemical Approaches to Unravel Stem Cell Biology*. *Stem Cell Reports*, 2018. **11**(6): p. 1312-1323.
75. Letai, A., P. Bhola, and A.L. Welm, *Functional precision oncology: Testing tumors with drugs to identify vulnerabilities and novel combinations*. *Cancer Cell*, 2022. **40**(1): p. 26-35.
76. Kitaeva, K.V., et al., *Cell Culture Based in vitro Test Systems for Anticancer Drug Screening*. *Frontiers in Bioengineering and Biotechnology*, 2020. **8**.
77. Newman, D.J. and G.M. Cragg, *Natural Products as Sources of New Drugs over the Nearly Four Decades from 01/1981 to 09/2019*. *Journal of Natural Products*, 2020. **83**(3): p. 770-803.
78. Thornburg, C.C., et al., *NCI Program for Natural Product Discovery: A Publicly-Accessible Library of Natural Product Fractions for High-Throughput Screening*. *ACS Chemical Biology*, 2018. **13**(9): p. 2484-2497.
79. Zhang, J.H., T.D. Chung, and K.R. Oldenburg, *A Simple Statistical Parameter for Use in Evaluation and Validation of High Throughput Screening Assays*. *J Biomol Screen*, 1999. **4**(2): p. 67-73.
80. Zwier, J.M., et al., *Image calibration in fluorescence microscopy*. *Journal of Microscopy*, 2004. **216**(1): p. 15-24.
81. Model, M.A. and J.K. Burkhardt, *A standard for calibration and shading correction of a fluorescence microscope*. *Cytometry*, 2001. **44**(4): p. 309-316.

Supplementary Fig 1
Results – Cellular uptake – TEOS-stabilized lipid multilayers are internalized by cells

